

Microstructure Control of Nanoporous Silica Thin Film Prepared by Sol-gel Process

Yiqun XIAO, Jun SHEN[†], Zhiyong XIE, Bin ZHOU and Guangming WU

Pohl Institute of Solid State Physics, Tongji University, Shanghai 200092, China

[Manuscript received June 12, 2006, in revised form October 23, 2006]

Nanoporous silica films were prepared by sol-gel process with base, acid and base/acid two-step catalysis. Transmission electron microscope (TEM) and particle size analyzer were used to characterize the microstructure and the particle size distribution of the sols. Scanning electron microscopy (SEM), atomic force microscopy (AFM) and spectroscopic ellipsometer were used to characterize the surface microstructure and the optical properties of the silica films. Stability of the sols during long-term storage was investigated. Moreover, the dispersion relation of the optical constants of the silica films, and the control of the microstructure and properties of the films by changing the catalysis conditions during sol-gel process were also discussed.

KEY WORDS: Sol-gel; Nanoporous; Microstructure; Optical constants

1. Introduction

It is well established by manufactures and users that optical coatings are generally prepared by physical vapor deposition (PVD) technology. Recently, sol-gel has become a new effective and competitive alternative method because of its low cost and simple operation. Sol-gel-derived silica films have many unusual properties such as adjustable refractive index, high porosity, controllable microstructure and high laser damage threshold. Besides, the sol-gel layer can be deposited in relatively thick layers and the chemical composition can be controlled precisely. Therefore it is becoming increasingly attractive for use in optical, microelectronic, magnetic and thermal applications such as anti-reflective coatings, thermal insulations^[1-6].

The nanoporous microstructure and properties of the silica films are greatly dependent on the experimental conditions during the sol-gel process. Up to now, a great deal of work has been done to control the microstructure and optical constants of silica films. Van Blaaderen *et al.*^[7] have investigated the growth mechanism and morphology of the silica particles in different solvents with various coatings. Labrosse and Burneau^[8] have prepared silica gels with different particle sizes in the range of 10–730 nm by hydrolysis and condensation of tetraethyl silicate (TEOS) with the catalysis of different concentrated ammonia solutions. Yoldas and Partlow^[9] have adjusted the refractive index of the films by controlling the proportion of water to alkoxide, concentration of alkoxide to solution, and a small amount of catalyst. Tong and Hu^[10] have reported an adjustment of the refractive index of the films using the same starting gel materials by controlling the aging of the gel. However, the control of the microstructure is not very convenient since there are too many concerned parameters.

The properties of silica films prepared by sol-gel process are closely related to the catalysis conditions. With the base catalysis, the silica film turns out to be a kind of nice optical material with low

optical constant, while its scratch resistance is relatively low. Whereas the silica film with acid catalysis has nice mechanism property, but it is too dense to have any porous structure, which results in a high optical constant and low laser-damage threshold^[11]. Inspiringly, base/acid two-step catalysis is a new route which can balance all these disadvantages mentioned above. The films from two-step catalyzed sols are widely used in the optical component of the high-power laser devices^[12], the composite functional films^[13], the antireflective films for the display systems^[14,15] and solar cells^[16,17]. In this paper, these three different catalysis conditions during the sol-gel process were used to control the nanoporous microstructure of silica films. The morphologies and properties were studied. The relation between the optical properties and microstructure of the films were discussed as well.

2. Experiments

2.1 Preparation of sol

The silica sols were synthesized using TEOS, ethanol and H₂O with base, acid and base/acid two-step catalysis, respectively.

For the base catalyzed sol, TEOS, NH₃·H₂O and ethanol were mixed at room temperature with a molar ratio of 1:2:40. Subsequently, the mixture was aged in a stable environment with humidity lower than 30% and temperature of 20–25°C for 7 d. After aging, the sol appeared to be Cambridge blue. The sol was then refluxed at 80°C for more than 10 h. Finally the sol was stored at 4°C.

For the acid catalyzed sol, TEOS, H₂O, ethanol and HCl were mixed at room temperature with a molar ratio of 1:2:40:10⁻³, and then the acid mixtures were aged in the stable environment (as mentioned above) for about 7 d.

For the base/acid two-step catalyzed sol, base catalyzed sol and acid catalyzed sol prepared above were stirred together, and subsequently were refluxed at 80°C for 10 h for further reaction and aging.

2.2 Preparation of film

Nanoporous silica films were prepared onto silicon

[†] Prof., Ph.D., to whom correspondence should be addressed, E-mail: Shenjj@online.sh.cn.

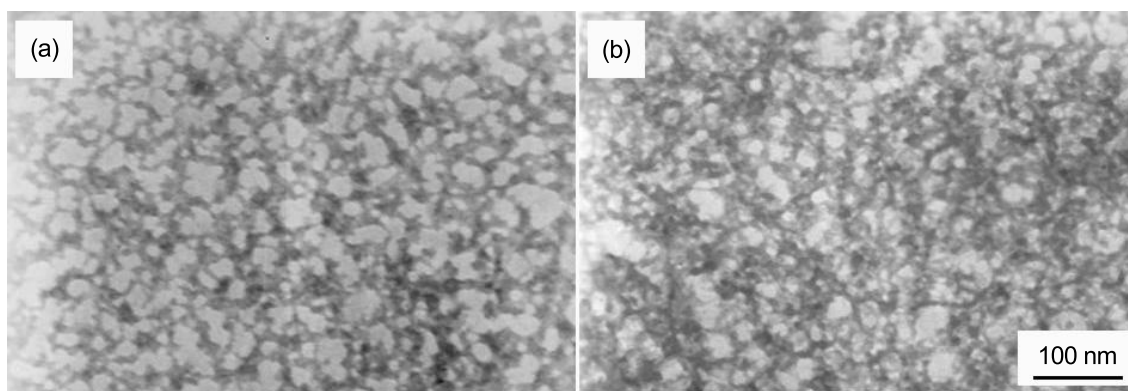


Fig.1 Transmission electron micrographs of the base catalyzed (a) and two-step catalyzed (b) silica sols

wafer and quartz glass using dip-coating in a clean room with humidity lower than 50% at room temperature. The coating device is CHEMAT DIPMASTER 200, and the coating speed could be varied from 0 to 13 inch/min (0 to 33.2 cm/min). Before coating the sol was treated in ultrasonicator for 30 min in order to separate the unstable aggregate. The film thickness was controlled by changing the drawing-speed during dip-coating process.

2.3 Post treatment

After coating, the films were placed in an ammonia atmosphere for 24 h, and subsequently heat-treated at 400°C for 2 h.

2.4 Characterization

Submicron particle size analyzer (COULTER N4PLU) was employed to measure the particle distribution of the silica sols. The network of the sols, cross-sectional and surface morphologies of the silica films were characterized by transmission electron microscopy (TEM, JEM-200CX), scanning electron microscopy (SEM, PHILIPS XL-30 FEC), and atomic force microscopy (AFM, PSIA Corporation XE-100). The refractive index and thickness of films were measured by a scanning spectroscopic ellipsometer (FUDAN ANZHEN Corporation, ELLIP-1).

3. Results

3.1 TEM observation

Figure 1 shows the TEM micrographs of the base catalyzed silica sol, and the base/acid two-step catalyzed sol which contains base and acid catalyzed sols with a volume ratio of 4:1. The base catalyzed sol has a complete cross-like network microstructure with an approximate average particle (or cluster) diameter of 10 nm. The interspaces which will eventually turn to be the pore of the film have an average size about 50 nm. It is clear that the network of the two-step catalyzed sol is quite similar to the base catalyzed sol, except that the particles are larger and the network is denser. Besides those, no network microstructure can be observed in the TEM photo of the acid catalyzed sol.

3.2 Stability of the sols

One of the crucial properties of the sols is the sta-

bility during long-term storage because the sols are needed for coating in a relatively long time. During the storage, the particles and clusters keep growing and the network keeps extending till the sol finally turns to be gel, which can not be used for coating. Moreover, the big size of particles and clusters would bring meso-scattering, which will influence the optical properties of the films dramatically.

The results of the experiments indicate that the sols are adapted for coating when the average particle size is below 100 nm. Under this condition, the optical properties, uniformity of structure and mechanism properties of the films are all sufficiently fine.

Figure 2 shows that the particle diameter distribution of the base and base/acid two-step catalyzed silica sols with different storage time. It can be readily observed that the base catalyzed sol was quite stable after the catalyst was wiped off by refluxing. The particle size had almost no change in a relatively long time, and the average particle diameter was about 11.5 nm after 60 d storage (see Fig.2(a)). As expected, the particle size of two-step catalyzed sol was larger due to the further cross linkage effect with acid catalysis after the sols were mixed. The average particle diameter was 52 nm after the sols were freshly mixed. Subsequently the particles in sol grew slowly due to the further activation of acid catalysis. After 150 d storage (see Fig.2(b)), the sol was still in a sufficient condition for coating. This indicates that the reaction during the sol-gel process was controlled with a relatively optimized condition. Besides, the acid catalyzed sol was extraordinary stable and could be used for coating in a whole year.

3.3 Optical properties

Figure 3 gives the wavelength-dependence of the refractive index in the visible region of the silica films with different catalysis. Cauchy model is presented well in fitting spectroscopic ellipsometric data for the optical constants. It is found that the refractive index of base catalyzed film varies from 1.20 to 1.21, while that of acid catalyzed film varies from 1.43 to 1.47. The extinction coefficient can be ignored since the values are quite small ($<10^{-3}$). The dispersion relations of these two kinds of films are very similar that the refractive index decreases exponentially as the wavelength increases. This also matches the dispersion relation of the compact bulk silica material

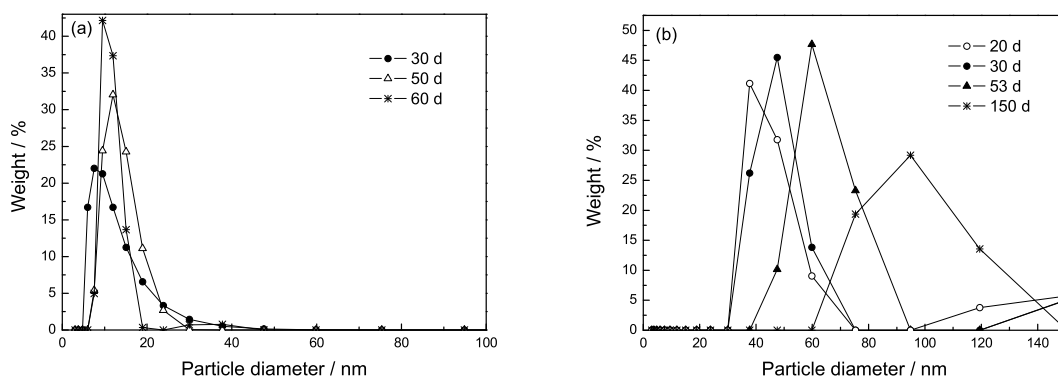


Fig.2 Particle diameter distribution of the base catalyzed (a) and base/acid two-step catalyzed (b) silica sols

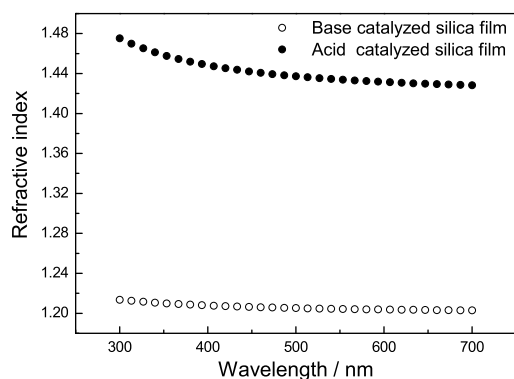


Fig.3 Optical constants of the silica film *via* sol-gel process with base catalysis and acid catalysis

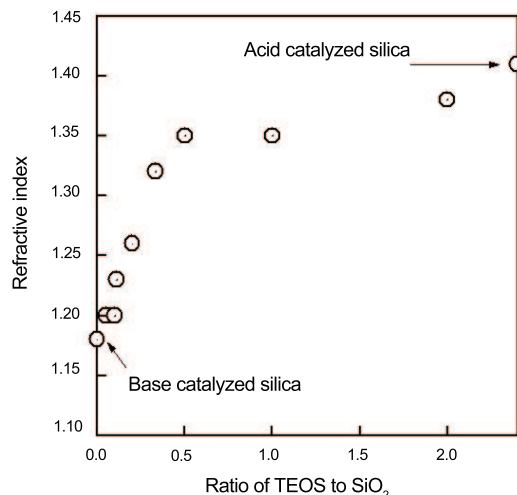


Fig.4 Relation between the refractive index of the silica films and the molar ratio of the acid TEOS mixture to the SiO₂ base catalyzed sol

well, though the values of the optical constants are quite different. As shown in Fig.4, the refractive index of the two-step catalyzed film varies between that of base and acid catalyzed film with the different mixing ratio of the base to the acid catalyzed sol. Higher ratio of the base catalyzed sol gives lower refractive

index, and vice versa. The value of the refractive index can be adjusted from 1.2 to 1.43.

3.4 Morphologies of the films

The surface morphologies of the silica films from the different sols are shown in Fig.5. It is found that the surface structure of the films is greatly dependent on the catalysis condition of the sols. The surface of film from base catalysis sol is considerably rough with a large quantity of large particles and clusters, which brings high porosity and loose structure, as shown in Fig.5(a); whereas the surface of the film from acid catalysis sol is very dense and smooth with small particles stacking together closely, as shown in Fig.5(b). The surface structure of two-step catalyzed film is similar with that of the base catalyzed films, except the particles are bigger.

4. Discussion

The difference in the microstructure of the films is related to the reaction speed of hydrolyzation and condensation during the sol-gel process^[18,19]. Under the acid catalysis conditions, hydrolysis is fast and condensation is slow. The growth of clusters can be described as a RLCA (Reaction Limited Cluster-cluster Aggregation) model. The growth tends to be linearly or randomly branched chains, and consequently the particles and clusters are sufficiently cross-linked (Fig.6(a)). Therefore, the formed film tends to be dense and the pore volume is extremely low. On the other hand, under the base catalysis conditions where hydrolysis is much slower than condensation, the aggregation finally tends to be DLCA (Diffusion Limited Cluster-cluster Aggregation). The growth tends to form a network of uniform spherical clusters with a large quantity of pores between them (Fig.6(b)). Therefore the film has a porous and loose structure. Under the base/acid two-step catalysis, when the sols with the linearly or randomly branched chain structure are doped into that with the spherical particle structure, the silica particles formed by the hydrolysis of the added TEOS with the acid catalysis in the second step can react with the surface hydroxyl groups of the silica particles formed in the first step, as shown in Fig.7. Therefore, the silica particles are bounded and the networks of the two-step catalyzed sols are denser than that of base catalyzed sols. Some

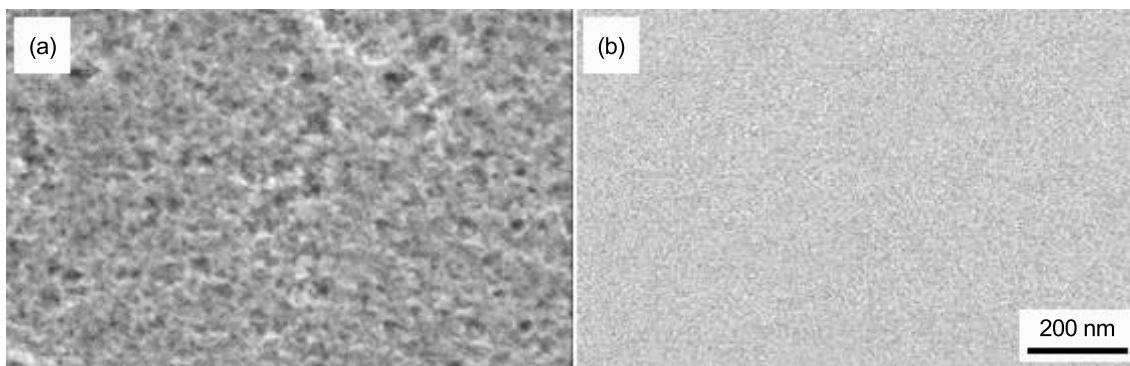


Fig.5 SEM pattern of surface morphology of the silica films *via* sol-gel process with base catalysis (a) and acid catalysis (b)

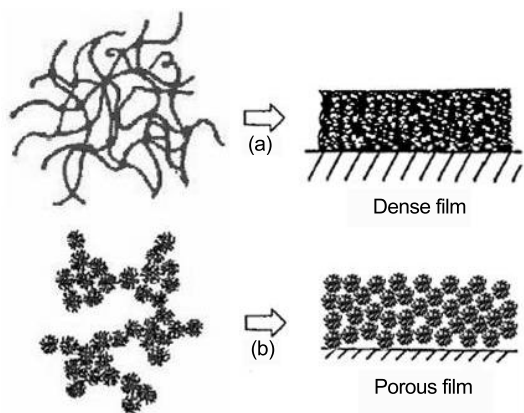


Fig.6 Schematic diagram of the formed network during sol-gel process with acid catalysis (a) and base catalysis (b)

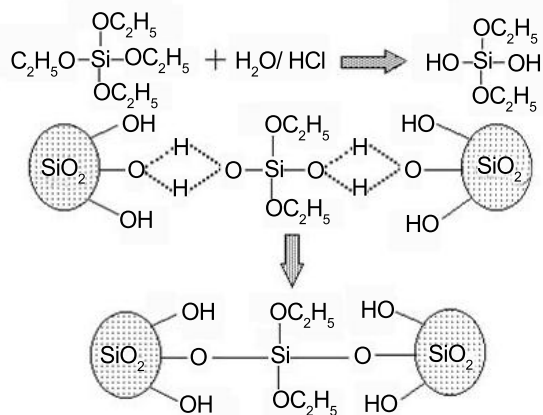


Fig.7 Schematic diagram of reaction mechanism for the base/acid two-step catalysis

pores are filled up and the porosity of the films from the two-step catalyzed sols can be adjusted between those two kinds. And the nanoporous structure can also be controlled by this way successfully. Moreover, after the second step catalysis, the mechanism properties of the base catalyzed silica film are greatly improved because the silica particles are bounded together firmly during this process. Besides, the adhesive force of the Si-O-Si chemical bonds for two-step

catalyzed film is much larger than that of the physical adsorption for base catalyzed film^[15], which results in a much better connection between film and substrate after the second step catalysis.

The refractive index of the nanoporous films is strongly related to the porosity of the films because of the following expression^[20]:

$$n_p^2 = (n^2 - 1)(1 - p) + 1$$

where n_p and n are the effective refractive index of the films and the refractive index of the compact silica bulk material, respectively, and p is the porosity of the porous film. It is obviously that the refractive index is inversely proportional to the root square of the porosity of the films. Hence the refractive index of acid catalyzed film is much higher than that of base catalyzed film. The refractive index of the two-step catalyzed film whose porous microstructure is controlled by the mixing ratio, therefore, can be varied from 1.20 to 1.43.

5. Conclusion

Nanoporous silica films were prepared by sol-gel process with base, acid and base/acid two-step catalysis successfully. It is concluded that the sols with optimized reaction conditions during the sol-gel process show sufficient stability in a long-term storage. Moreover, the microstructure of the sols and films can be well controlled by changing the catalysis conditions, as well as the optical and mechanical properties of the films can be controllably varied. The refractive index of the sol-gel derived silica film is adjusted between 1.20 and 1.43.

Acknowledgements

The authors are very grateful to the National Natural Science Foundation of China (Grant No. 20133040), the Chinese National Foundation of High Technology (2002AA842052), the Shanghai Nanotechnology Promotion Center (0352nm022, 0352nm056), and the Shanghai International Cooperation Program and Trans-Century Training Programme Foundation for the Talents by the State Education Commission.

REFERENCES

[1] G.M.Wu, J.Wang and J.Shen: *J. Phys. D Appl.*

- Phys.*, 2001, 1301.
- [2] I.M.Thomas: *Appl. Optics*, 1992, **31**(28), 6145.
- [3] S.M.Attia, J.Wang, G.M.Wu, J.Shen and J.H.Ma: *J. Mater. Sci. Technol.*, 2002, **18**(3), 211.
- [4] Y.P.Zhang, X.Y.Wang, H.P.Xia, D.F.Shen, F.X.Gan, S.Y.Wang and L.Y.Chen: *J. Mater. Sci. Technol.*, 2004, **20**(1), 66.
- [5] C.J.Brinker, A.J.Hurd, P.R.Schunk, G.C.Frye and C.S.Ashley: *J. Non-Cryst. Solids*, 1992, **147/148**, 424.
- [6] Y.Zhang, D.Wu, Y.H.Sun and S.Y.Peng: *J. Sol-Gel Sci. Technol.*, 2005, **33**, 19.
- [7] A.Van Blaaderen, J.Van Geest and A.Vrij: *J. Colloid Interf. Sci.*, 1992, **154**, 481.
- [8] A.Labrosse and A.Burneau: *J. Non-Cryst. Solids*, 1997, **221**, 107.
- [9] B.E.Yoldas and D.P.Partlow: U.S. Patent No.4535026, 1985.
- [10] H.S.Tong and C.M.Hu: U.S. Patent No.5582859, 1996.
- [11] I.M.Thomas: *Appl. Optics*, 1986, **25**(9), 1481.
- [12] Yiqun XIAO, Jun SHEN, Lanfang YAO, Shan WANG and Fan YANG: *High Power Laser and Particle Beams*, 2004, **16**(10), 1281. (in Chinese)
- [13] J.Liu, F.Shi and D.Yang: *J. Mater. Sci. Technol.*, 2004, **20**(5), 550.
- [14] G.M.Wu, J. Shen, T.H.Yang, B.Zhou and J.Wang: *J. Mater. Sci. Technol.*, 2003, **19**(4), 299.
- [15] K.Koc, F.Z.Tepehan and G.G.Tepehan: *J. Mater. Sci.*, 2005, **40**, 1363.
- [16] M.C.Bautista and A.Morales: *Solar Energy Mat. Sol. C.*, 2003, **80**, 217.
- [17] P.Nostell, A.Roos and B.Karlsson: *Thin Solid Films*, 1999, **351**, 170.
- [18] R.B.Pettit, C.S.Ashley, S.T.Reed and C.J.Brinker: *Sol-Gel Technology for Thin Films, Fibers, Preforms, Electronics and Speciality Shapes*, ed. by L.C.Klein, Noyes Publications, Park Ridge, New Jersey, 1987, 80.
- [19] Jun SHEN, Jue WANG and Xiang WU: *Physics*, 1994, **23**(8), 483. (in Chinese)
- [20] Guangming WU, Tianhe YANG, Jue WANG, Jun SHEN, Tianhe YANG, Zhenquan LAI, Huilin ZHANG and Qinyuan ZHANG: *Atom. Energy Sci. Technol.*, 1999, **33**(4) 332. (in Chinese)